Cancer Research

CRLX101, a Nanoparticle–Drug Conjugate Containing Camptothecin, Improves Rectal Cancer Chemoradiotherapy by Inhibiting DNA Repair and HIF1α

Xi Tian[1], Minh Nguyen[1], Henry P. Foote[1], Joseph M. Caster[1], Kyle C. Roche[1], Christian G. Peters[2], Pauline Wu[2], Lata Jayaraman[2], Edward G. Garmey[2], Joel E. Tepper[1], Scott Eliasof[2], and Andrew Z. Wang[1]

Abstract

Novel agents are needed to improve chemoradiotherapy for locally advanced rectal cancer. In this study, we assessed the ability of CRLX101, an investigational nanoparticle–drug conjugate containing the payload camptothecin (CPT), to improve therapeutic responses as compared with standard chemotherapy. CRLX101 was evaluated as a radiosensitizer in colorectal cancer cell lines and murine xenograft models. CRLX101 was as potent as CPT *in vitro* in its ability to radiosensitize cancer cells. Evaluations *in vivo* demonstrated that the addition of CRLX101 to standard chemoradiotherapy significantly increased therapeutic efficacy by inhibiting DNA repair and HIF1α pathway activation in tumor cells. Notably, CRLX101 was more effective than oxaliplatin at enhancing the efficacy of chemoradiotherapy, with CRLX101 and 5-fluorouracil producing the highest therapeutic efficacy. Gastrointestinal toxicity was also significantly lower for CRLX101 compared with CPT when combined with radiotherapy. Our results offer a preclinical proof of concept for CRLX101 as a modality to improve the outcome of neoadjuvant chemoradiotherapy for rectal cancer treatment, in support of ongoing clinical evaluation of this agent (LCC1315 NCT02010567). *Cancer Res; 77(1); 112–22. ©2016 AACR.*

Introduction

It is estimated that 40,000 patients are diagnosed with rectal cancer, and that approximately 22,000 patients die from this disease in the United States each year (1). Although some patients present with early disease that can be cured with surgical resection alone, many patients present with locally advanced disease (T3 and/or N+) that requires neoadjuvant chemoradiotherapy (CRT) followed by surgical resection (2). The standard neoadjuvant CRT regimen consists of administering either infusional 5-fluorouracil (5-FU) or oral capecitabine with approximately 50 Gy of radiotherapy to the pelvis. In addition to neoadjuvant CRT, postoperative CRT has also proved beneficial (3). A few clinical trials have shown that rectal cancer patients receiving CRT after surgical resection demonstrate reduced rates of local recurrence and improved survival when compared with patients receiving surgery alone (4–6). For these reasons, CRT represents an important treatment strategy for rectal cancer.

A number of studies have suggested that CRT alone may be an effective rectal cancer treatment strategy. Several large randomized trials have demonstrated that 8% to 25% of patients receiving only CRT achieve a pathologic complete response (pCR; refs. 7–13). Importantly, patients who achieve a pCR also achieve improved overall and recurrence free survival (14–16). Moreover, recent clinical studies have suggested that surgery can be omitted in patients with pCR to preserve organ integrity and quality of life (17). Therefore, identifying therapeutic agents that can be combined with standard CRT to improve the pCR rates of rectal cancer patients has been an active area of research (18).

Many clinical trials have evaluated whether pCR rates of CRT can be improved via the inclusion of additional therapeutic agents to 5-FU and radiotherapy. Specifically, trials have evaluated the effect of adding chemotherapeutics (oxaliplatin and irinotecan) and targeted antibodies (bevacizumab and cetuximab) to standard CRT. Clinical studies evaluating the addition of oxaliplatin to standard CRT showed increased toxicity with no added therapeutic benefit (12, 19). Although some trials have shown that the addition of irinotecan improves pCR rates in rectal cancer patients (20), the clinical adoption of this treatment strategy was prevented by unacceptable off-target toxicity (21, 22). The use of targeted therapies such as bevacizumab and cetuximab with standard CRT has yielded mixed results and, therefore, has not been integrated into standard treatment regimens (9). Consequently, there remains great interest in the development of novel agents that can be

[1]Department of Radiation Oncology, Lineberger Comprehensive Cancer Center, Carolina Center for Cancer Nanotechnology Excellence, Carolina Institute of Nanomedicine, University of North Carolina at Chapel Hill, Chapel Hill, North Carolina. [2]Cerulean Pharma Inc., Waltham, Massachusetts.

Note: Supplementary data for this article are available at Cancer Research Online (http://cancerres.aacrjournals.org/).

Corresponding Author: Andrew Z. Wang, University of North Carolina at Chapel Hill, CB 7512, UNC Chapel Hill, Chapel Hill, North Carolina, 27514. Phone: 984-974-8425; Fax: 984-974-8607; E-mail: zawang@med.unc.edu

doi: 10.1158/0008-5472.CAN-15-2951

combined with established CRT regimens to improve rectal cancer treatment.

Inhibitors of topoisomerase 1 (topo-1), including the marketed drugs irinotecan and topotecan, are well-known radiosensitizers (23). Irinotecan is highly effective against colorectal cancer, but it produces unacceptable gastrointestinal (GI) toxicity when combined with radiotherapy (20). Camptothecin (CPT) has been shown to be an effective treatment for rectal cancer in preclinical studies, but it could not be developed clinically because it was not well tolerated. The recent clinical development of CRLX101, an investigational nanoparticle–drug conjugate containing the payload CPT, offers a unique opportunity to improve CRT for rectal cancer. CRLX101 is a nanoparticle consisting of CPT (10% by weight) conjugated to a biocompatible copolymer of cyclodextrin and polyethylene glycol (PEG; ref. 24). CRLX101 nanoparticles have diameters ranging from 20 to 30 nm and a slightly negative ζ-potential (−5 mV; ref. 24). Physiologically, CRLX101 has been shown to be a potent inhibitor of topo-1 and hypoxia-inducible factor-1 alpha (HIF1α), a signaling molecule that promotes radioresistance in cancer cells (24–26). Currently, CRLX101 is being evaluated in phase II trials as both a monotherapy and in combination with other anticancer drugs as a treatment strategy for several tumor types (27).

CRLX101 has several attractive properties that may improve CRT. First, CRLX101, as a nanoparticle, preferentially accumulates in tumors through the enhanced permeability and retention (EPR) effect (28, 29). Secondly, CRLX101 has not demonstrated any significant GI toxicity to date (27, 30). Thirdly, CRLX101 has a long circulation time (circulation half-life of 17.2 hours; ref. 31). In addition, CRLX101 releases CPT in a prolonged fashion, which is particularly conducive for radiosensitization during fractionated radiotherapy (16). Lastly, CRLX101 has the potential to promote radiosensitization through two independent mechanisms, inhibition of topo-1 and HIF1α (25).

Given the radiosensitizing potential that CPT has demonstrated in preclinical studies, we hypothesized that the efficacy of standard CRT would be significantly improved by the addition of CRLX101. Therefore, we evaluated whether the addition of CRLX101 to 5-FU and radiotherapy could improve rectal cancer treatment using preclinical rectal cancer models. Our study supports the ongoing clinical investigation of CRLX101 in rectal cancer CRT.

Materials and Methods

Materials

CRLX101 was provided by Cerulean Pharma Inc. Each gram of CRLX101 contained 100 mg of CPT. CRLX101 was resuspended in phosphate buffer saline. CPT was purchased from ACROS Organics. 5-FU and oxaliplatin were purchased from Sigma-Aldrich.

Mice

Nu/Nu mice (male, 7–8 weeks old) were obtained from the animal colony at the University of North Carolina (UNC) Lineberger Comprehensive Cancer Center (LCCC). C57BL/6J mice (male, 8 weeks old) were purchased from The Jackson Laboratory. All animal experiments were performed in accordance with guidelines from the UNC Institutional Animal Care and Use Committee.

Cell culture

Human colorectal cancer cell lines HT-29 (ATCC batch F-9246) and SW480 cells (ATCC batch 7265) were obtained from the Tissue Culture Facility at the LCCC at UNC in 2014. Cell line authentication was performed via short tandem repeat in 2014. The luciferase-expressing cell line HT-29-luc2 was purchased from Caliper Life Sciences in 2014. All cell lines were used within 10 passages after initial plating. HT-29, SW480, and HT-29-luc2 cells were cultured at 37°C in 5% CO_2 humidified atmosphere in Dulbecco's Modified Eagle Medium: Nutrient Mixture F-12 (DMEM/F12; Gibco) supplemented with 10% (vol/vol) fetal bovine serum (Gibco) and 1% penicillin/streptomycin (Gibco).

X-Ray irradiation

Cells and mice were irradiated using a Precision X-RAD 320 (Precision X-Ray, Inc.) machine operating at 320 kVp and 12.5 mA. For tumor growth assays, a 3-mm lead shield protected the mice's vital organs, and the left flank remained exposed during irradiation. In order to test hair loss toxicity, a 0.5-cm thick bolus covered the left dorsal region of the mice during irradiation to enhance the skin dose. For GI toxicity, the entire pelvic region was irradiated while a 3-mm lead shield protected the legs, upper abdomen, thoracic region, and head of the mouse.

Cell viability assay

Cells were seeded at 10,000 cells/well in 96-well plates. Cells were treated with CRLX101, CPT, or PBS (control) for 24 hours, washed with PBS after incubation, and incubated in fresh, complete medium for 24 hours. Following incubation, MTS [(3-(4,5-dimethylthiazol-2-yl)-5-(3-car-boxymethoxyphenyl)-2-(4-sulfophenyl)-2H-tetrazolium)] cell proliferation assays were performed according to the manufacturer's protocols using the CellTiter 96 Aqueous One Solution Cell Proliferation assay kit (Promega).

Clonogenic assay

A monolayer of cancer cells was treated with 10 μmol/L CRLX101 (CPT equivalents), 10 μmol/L CPT, or PBS (control) for 24 hours, washed with fresh media, and then irradiated at 0, 1, 2, 4, or 6 Gy. After treatment, cells were plated into 25 mL flasks at densities ranging from 100 to 250,000/plate. Cells were incubated for 13 days, fixed, and then stained with 4% formaldehyde/80% methanol/0.25% crystal violet (Fisher Scientific). All colonies containing 30 or more cells were counted. Plating efficiency (PE) was determined for each cell line. Surviving fraction (SF) was calculated using the formula [# of colonies/(# of plated cells) (PE)]. SF was plotted against radiation dose on a log scale. The linear-quadratic formula [$SF = e^{-\alpha D-\beta D^2}$] was used to generate survival curves using R package "CFAssay."

In vitro histone H2AX phosphorylation and HIF1α inhibition

HT-29 cells were irradiated with 2 Gy, washed with PBS, and then treated with 10 μmol/L CPT, CRLX101, or PBS (control) diluted in culture medium. After 1, 12, or 48 hours, the cells were processed for either immunofluorescence or Western blot analysis.

Western blot

Cells were lysed in RIPA lysis buffer [25 mmol/L Tris–HCl (pH 7.6), 150 mmol/L NaCl, 1% NP-40, 1% sodium deoxycholate, 0.1% SDS] supplemented with a protease and phosphatase inhibitor cocktail (Thermo Scientific) at the indicated times after irradiation. Protein concentration was determined using bicinchoninic acid protein assay (Pierce). The primary antibodies used

were anti-Human HIF1α (Novus Biologicals, cat #NB100-479), VEGF (A-20; Santa Cruz Biotechnology, cat #sc152), and β-Actin (Cell Signaling Technology, cat #4970). The secondary antibodies used were anti-Rabbit or anti-Mouse IgG HRP-linked antibodies (Cell Signaling Technology). The intensity of protein bands on the Western blot image was quantified using ImageJ software. Ratios of HIF1α and VEGF protein levels after β-actin normalization were calculated from three independent experiments.

Immunofluorescence

Cells were fixed in 4% formaldehyde for 30 minutes, rinsed with PBS, and incubated in goat blocking solution (2% goat serum, 1% BSA, 0.1% Triton X-100, and 0.05% Tween 20) or 5% BSA blocking solution for 1 hour. After blocking, cells were stained with anti-human HIF1α (BD Transduction Laboratories, cat #610958) or anti-phospho-histone H2AX (Ser139) antibodies (Millipore, cat #05-636) for 1 hour at room temperature. Cells were then washed with PBS and further incubated with secondary antibody Alexa Fluor 568 Goat anti-Mouse IgG antibody (Molecular Probes, cat #A11004) or Alexa Fluor 594 Donkey anti-Mouse IgG antibodies (Molecular Probes, cat #A21203) for 30 minutes. After washing, cells were mounted using ProLong Gold Antifade Mountant with DAPI (Molecular Probes, cat #P36935). HIF1α immunofluorescent images were acquired using an Olympus BX61 fluorescence microscope (40× objective lens). γH2AX immunofluorescent images were acquired using a Zeiss LSM 700 laser scanning confocal microscope with z-stack sectioning (63× oil immersion objective lens). To minimize the overlap of foci, images were stacked by maximum intensity projection. The number of γH2AX foci per cell was counted using ImageJ software.

Immunohistochemistry of tissue sections

For immunohistochemical studies of tumor xenografts, HT-29 cells (1×10^6 cells in 200 μL in 1:1 DMEM/F12 and Matrigel) were inoculated subcutaneously into the left dorsal flanks of 8-week-old male Nu/Nu mice. Eleven days after inoculation, mice were treated with CRLX101 (5 mg/kg), CPT (5 mg/kg), or PBS (control) and given a single 5 Gy dose of radiation 1 hour later. Mice were sacrificed at 1 and 7 days after radiation treatment, and tumor samples were harvested for histology. Tumors were fixed in 4% formaldehyde for 24 to 48 hours at 4°C, paraffin embedded, and cut into 6-μm sections. For GI toxicity assays, colons were flushed with PBS and fixed overnight in 4% PFA. Tissues were then transferred to 30% sucrose for 24 hours, cut longitudinally, "swiss rolled," and embedded in optimal cutting temperature (OCT) compound. Using a cryotome, 8-μm sections of OCT-embedded tissues were taken and placed onto microscope slides. Sections were immersed in blocking solution (2% goat serum, 1% BSA, 0.1% Triton X-100, and 0.05% Tween 20) for 1 hour. After blocking, sections were incubated with primary antibodies overnight at 4°C. Three primary antibodies were used: carbonic anhydrase 9 (CAIX) antibody (H-120; Santa Cruz Biotechnology, sc-25599), VEGF antibody (A-20; Santa Cruz Biotechnology, sc-152), and cleaved caspase-3 (Asp175; Cell Signaling Biotechnology, 9661). The secondary antibodies used were Alexa Fluor 594 Goat anti-Rabbit IgG antibody or Alexa Fluor 568 Goat anti-mouse IgG antibody (Molecular Probes). Slides were mounted using ProLong Gold Antifade Mountant with DAPI (Molecular Probes, cat #P36935). Images were acquired using a Zeiss LSM 700 confocal microscope.

GI toxicity

C57BL/6J mice were intravenously (i.v.) injected with 1 dose of CRLX101 (5 mg/kg), CPT (5 mg/kg), or PBS (control) and given 3 fractions of radiation at 5 Gy daily (15 Gy total). Tissues were then collected, processed, and stained for cleaved caspase-3. Toxicity was evaluated at 2, 4, and 14 days after treatment by quantifying the number of cleaved caspase-3–positive cells per crypt unit. A minimum of 50 crypt units were quantified for each sample.

Hair toxicity

C57BL/6J mice were i.v. injected with a single i.v. dose of CRLX101 5 mg/kg), CPT (5 mg/kg), or PBS (control) and sequentially subjected to a radiation dose of 15 Gy (1 fraction). After 49 days, mice were evaluated for hair loss.

***In vivo* drug efficacy**

Tumors were established by subcutaneous injection of cancer cells suspended in 200 μL 1:1 DMEM:F12 and Matrigel into the left dorsal flank of 6- to 8-week-old male Nu/Nu mice. For HT-29 tumor xenografts, 1×10^6 cells were injected. For SW480 tumor xenografts, 2.5×10^6 cells were injected. Treatment began 10 days after tumor inoculation, or when tumors reached 100 to 150 mm^3. Mice were weighed and randomly sorted into treatment groups (8–10 mice per group). To evaluate drug efficacy of CRLX101 as a radiosensitizer *in vivo*, a single dose of CRLX101 (5 mg/kg) with or without 5-FU (20 mg/kg) was administered by tail-vein i.v. injection. To evaluate CRLX101 plus 5-FU combined chemoradiotherapy with other combination regimens, CRLX101 (5 mg/kg), oxaliplatin (16.7 mg/kg, equivalent to 50 mg/m^2 in human), and/or 5-FU (20 mg/kg) were administered to tumor-bearing mice via tail-vein i.v. injection. Mice were irradiated with three fractions of radiation at 5 Gy (15 Gy total) daily. The first fraction of radiation was administered 1 hour after injection. Tumor volumes were determined by measuring two perpendicular diameters, a and b, using the formula $[V = 0.5 \times a \times b^2]$ (a and b represent the long and short perpendicular diameters, respectively). Measurements were recorded every 2 to 3 days using a digital caliper. The relative tumor size was defined by V/V_0, where V represents the tumor volume over time and V_0 represents the initial tumor volume. Mice were euthanized when the tumor volume reached 5 times the initial volume.

Cell repopulation assay

HT-29 cells were treated with CRLX101 (37.5 ng/mL), 5-FU (0.15 μg/mL), CRLX101 + 5-FU (37.5 ng/mL and 0.15 μg/mL, respectively), or PBS (control) for 48 hours and irradiated with 4 Gy. After treatment, 1×10^5 treated HT-29 cells were mixed and seeded with 1,000 untreated HT-29-luc2 cells in 6-well plates. Luciferase activity was recorded every 2 to 3 days over 13 days using IVIS Kinetic Optical System (Caliper Life Sciences). Images were taken 10 minutes after adding D-luciferin substrate solution (System Biosciences).

Statistical analysis

Results from histological analysis, Western blot assays, and MTS assays were statistically assessed by either one-way or two-way ANOVA followed by Tukey honestly significant difference *post hoc* test (if a positive F test was detected). For clonogenic assays, linear-quadratic cell survival curves were analyzed using R package "CFAssay." For tumor growth curve and luciferase activity experiments, we used area under the growth curve (AUC).

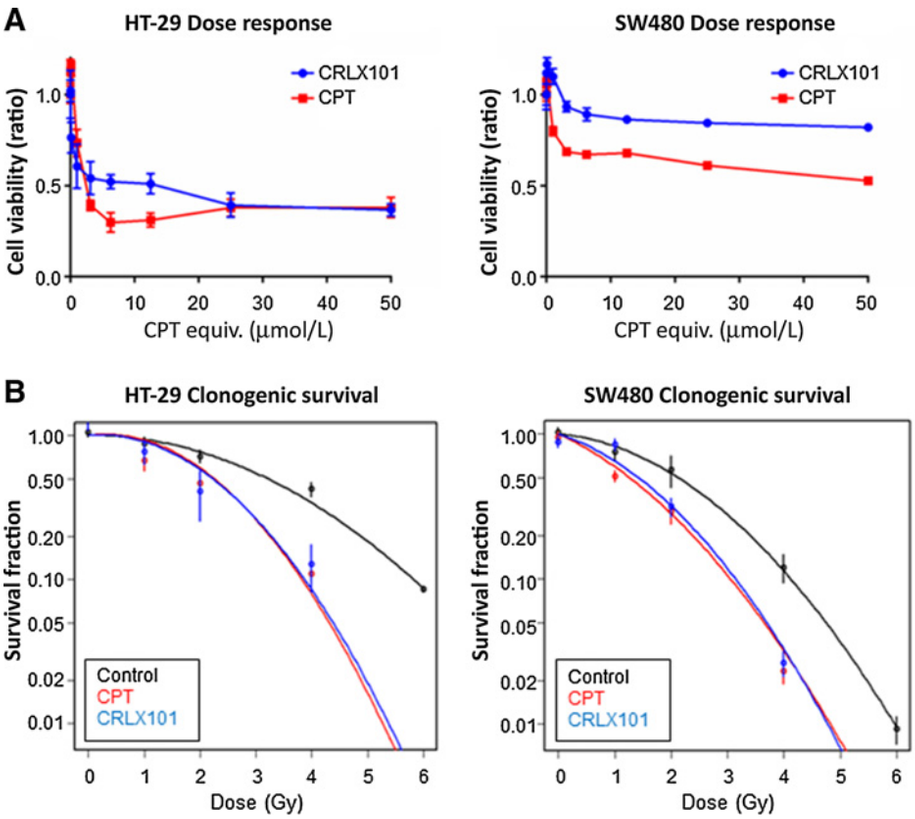

Figure 1.
Direct cytotoxicity and radiosensitization potential of CRLX101 treatment *in vitro*. **A,** Cell viability of HT-29 and SW480 cells following 24 hours of CRLX101 or CPT treatment. **B,** Clonogenic survival curves of HT-29 and SW480 cells treated with CRLX101 or CPT and radiation.

The Wilcoxon rank sum test was used to compare the growth rates as previously described (32). *P* values less than 0.05 were considered statistically significant.

Results

CRLX101 is a potent radiosensitizer *in vitro*

CRLX101 was evaluated as a radiosensitizer *in vitro* using two colorectal cancer cell lines: HT-29 and SW480. To determine the direct cytotoxic impact of CRLX101 on each cell line, we generated dose–response curves in the absence of radiation (Fig. 1A). We found that the direct cytotoxicity of CRLX101 was generally lower than the cytotoxicity of CPT. The IC_{50} values of CRLX101 were higher for both HT-29 and SW480 cells. Additionally, SW480 cells treated with CRLX101 demonstrated higher rates of survival across all treatment concentrations when compared with cells treated with CPT (Fig. 1A). We then compared the radiosensitizing effects of CRLX101 and CPT using radiation survival curves. We found that CRLX101 and CPT both act as potent radiosensitizers in HT-29 and SW480 cells (Fig. 1B). Sensitization enhancement ratios (SER) were calculated as the ratio of doses required to achieve 10% surviving fraction of cells. The SERs for CPT were 2.2 for HT-29 and 1.5 for SW480. At equivalent drug concentrations, the SERs for CRLX101 were 2.3 for HT-29 and 1.3 for SW480.

CRLX101 inhibits DNA damage repair

The induction of DNA double-strand breaks (DSB) by ionizing radiation or cytotoxic agents causes histone variant H2AX to become rapidly phosphorylated at serine 139 (γH2AX) and to form discrete nuclear foci. To examine if CRLX101 inhibits DNA repair following radiation damage, γH2AX foci formation and persistence was analyzed using immunofluorescence. At 1 hour following radiation damage, we observed equivalent γH2AX foci formation in all treatment conditions (Fig. 2A). At 12 hours following radiation damage, we observed a significant decrease in the number of γH2AX foci in untreated control cells, suggesting successful DNA repair. In contrast, we observed an increase in the number of γH2AX foci in cells treated with either CRLX101 or CPT ($P < 0.001$; Fig. 2B). These results indicate that CRLX101 and CPT promote radiosensitization by directly inducing additional DNA damage and/or inhibiting DNA repair.

CRLX101 inhibits radiation induced HIF1α activation *in vitro* and *in vivo*

Cancer cells evade radiation-induced apoptosis in part through activation of HIF1α signaling (33, 34). To examine the effect that CRLX101 has on HIF1α signaling after radiation damage, we assessed HIF1α expression levels in HT-29 cells following radiotherapy. At 1 hour following radiation damage, control cells and cells treated with either CRLX101 or CPT all demonstrated similar HIF1α expression levels (Fig. 3A and B). At 12 hours following radiation damage, however, the expression of HIF1α was significantly lower in cells treated with either CPT or CRLX101 when compared with levels of HIF1α present in control cells (Fig. 3A). We found that the expression of HIF1α was suppressed by CRLX101 for at least 48 hours, as shown by Western blot analysis (Fig. 3B).

HIF1α directly upregulates the expression of genes that are involved in tumor angiogenesis (e.g., VEGF), pH balance (e.g., CAIX), and glucose metabolism (25, 35). To determine the effect

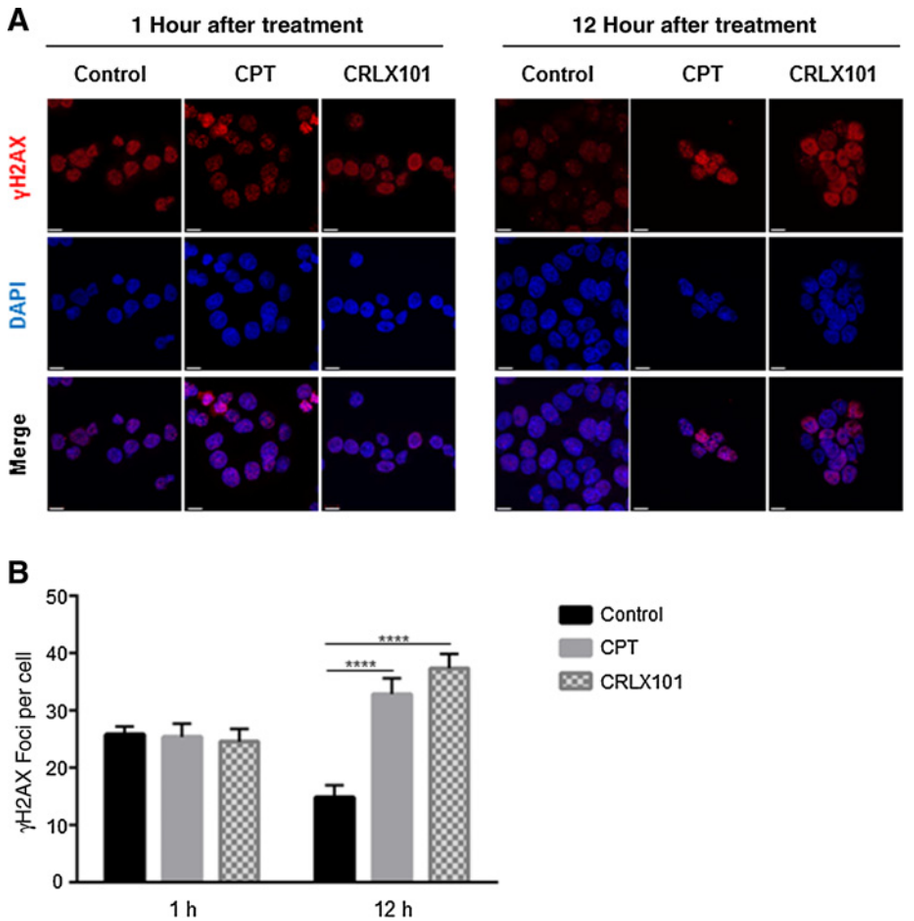

Figure 2.
Effect of CRLX101 treatment on radiation-induced DSB repair. **A,** γH2AX foci formation (red) in nuclei (blue) of HT-29 cells following treatment with radiation and PBS (control), CPT, or CRLX101. Scale bar, 10 μm. **B,** Quantification of the number of γH2AX foci present in **A**. ****, $P < 0.001$.

of CRLX101 on downstream HIF1α signaling, we assessed the expression of VEGF and CAIX in tumors using immunofluorescence. Mice bearing HT-29 xenograft tumors were treated with CRLX101, CPT, or PBS (control) and then irradiated. One day following treatment, we observed similar levels of VEGF expression in tumors from control animals and animals treated with either CPT or CRLX101 (Fig. 3C). Seven days following treatment, however, we found that tumors from mice treated with either CPT or CRLX101 showed significantly less VEGF expression when compared with tumors taken from control animals (Fig. 3D). In addition to VEGF expression, we also assessed the expression of CAIX. We found that tumors from control animals and animals treated with CPT demonstrated prominent CAIX expression at 1 and 7 days after treatment. In contrast, we found that tumors from animals treated with CRLX101 demonstrated a modest reduction of CAIX expression 1 day after treatment followed by a more prominent reduction of CAIX expression at 7 days after treatment (Fig. 3C and D).

CRLX101 is a potent radiosensitizer and improves 5-FU–based rectal cancer chemoradiotherapy in xenograft models

We next sought to evaluate the efficacy of CRLX101 as a radiosensitizer *in vivo*. Given that 5-FU is part of the standard CRT regimen for rectal cancer, we assessed the therapeutic efficacies of combining radiotherapy with CRLX101, 5-FU, or CRLX101 and 5-FU using murine rectal cancer xenograft models. We chose a flank xenograft model over an orthotopic model for the ease of measuring tumor volume over time. Immunodeficient mice bearing either HT-29 or SW480 xenografts were treated with a single dose of chemotherapy followed by three daily fractions of radiotherapy (5 Gy × 3). In SW480 xenografts, radiotherapy combined with CRLX101 delayed tumor growth more than radiotherapy combined with 5-FU (CRLX101 + XRT vs. 5-FU + XRT: $P = 0.0006$; Fig. 4B). In mice bearing HT-29 tumor xenografts, the greatest therapeutic efficacy was observed when CRLX101 and 5-FU were combined with radiotherapy (5-FU + CRLX101 + XRT vs. CRLX101 + XRT: $P = 0.001$; Fig. 4A). Our results show that the addition of CRLX101 to 5-FU–based CRT significantly improves the therapeutic index.

While oxaliplatin has been studied extensively in rectal cancer CRT, clinical studies suggest that it does not enhance the therapeutic index of standard CRT regimens. To determine whether CRLX101 enhances standard rectal cancer CRT more than oxaliplatin, we assessed the therapeutic efficacies of combining radiotherapy with 5-FU, 5-FU and oxaliplatin, and 5-FU and CRLX101 using HT-29 and SW480 murine xenograft models. As shown in Fig. 4C and 4D, the slowest tumor growth was observed in animals treated with radiotherapy and both 5-FU and CRLX101. Consistent with clinical studies, the addition of oxaliplatin to 5-FU CRT did not improve the therapeutic efficacy of standard CRT. These data suggest that CRLX101 acts synergistically with 5-FU to suppress tumor growth.

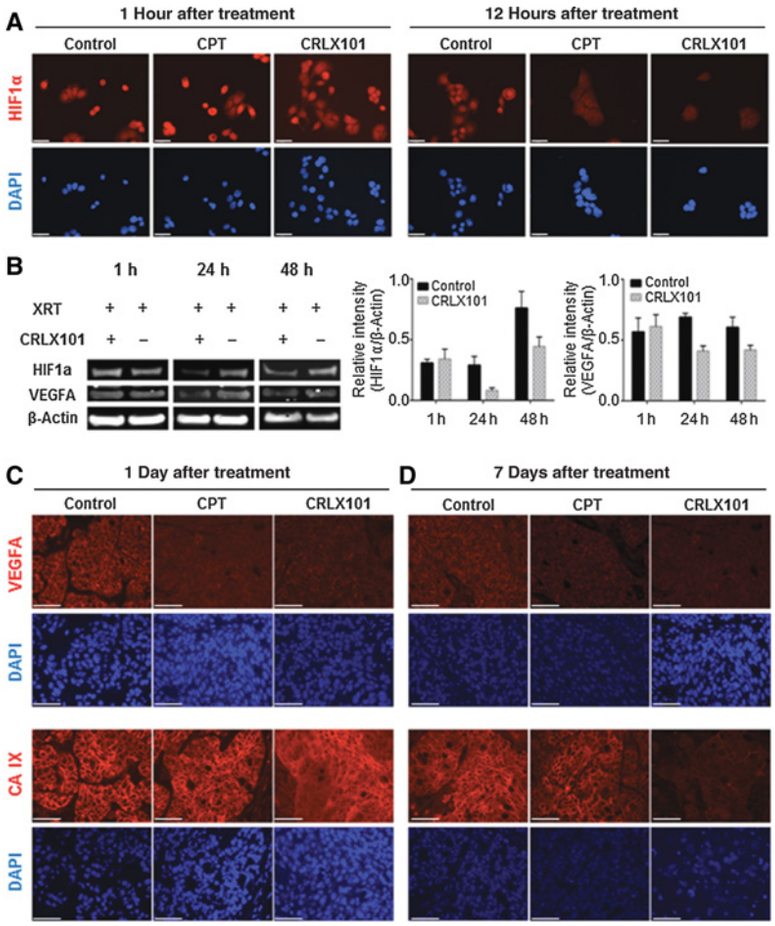

Figure 3.

Effect of CRLX101 on HIF1α signaling following radiation. **A,** Time course of HIF1α expression (red) in the nuclei (blue) of HT-29 cells following treatment with radiotherapy and PBS (control), CPT, or CRLX101. Scale bar, 16 μm. **B,** Quantification of HIF1α and VEGFA protein expression in HT-29 cells at various time points following treatment with radiation and PBS (control) or CRLX101. **C–D,** VEGFA and CAIX expression in xenograft tumors at 1 and 7 days after animals were treated with radiation and PBS (Control), CPT, or CRLX101. Scale bar, 50 μm.

5-FU can inhibit tumor repopulation after CRLX101-based CRT

To determine why the combination of CRLX101 and 5-FU CRT had the highest therapeutic efficacy *in vivo*, we examined the effect of different CRT regimens on repopulation rates of untreated HT-29 cells *in vitro* using a previously established repopulation assay (36). Briefly, we mixed a small number of untreated, luciferase-labeled HT-29 (HT-29-luc2) cells with a larger number of treated, unlabeled HT-29 cells and assessed the growth rate of untreated HT-29-luc2 cells via luciferase activity over time (Fig. 5A). Note that there is a strong linear correlation between bioluminescence and HT-29-luc2 cell numbers ($R^2 = 0.9953$; Supplementary Fig. S1). When compared with cells treated with PBS or 5-FU plus radiation, cells treated with CRLX101 and radiation or the combination of CRLX101, 5-FU, and radiation significantly increased the proliferation rate of cocultured untreated HT-29-luc2 cells (Fig. 5B). These results indicate that cells treated with CRLX101 or CRLX101 and 5-FU promote accelerated repopulation. Importantly, untreated HT-29-luc2 cells cocultured with cells treated with 5-FU and CRLX101 demonstrated a lower proliferation rate when compared with cells cocultured with cells treated with CRLX101 alone ($P = 0.049$; Fig. 5B and C). These results suggest that by limiting accelerated cell repopulation, the combination of CRLX101, 5-FU, and radiation has a greater therapeutic efficacy than CRLX101 plus radiation *in vivo*.

CRLX101 has low *in vivo* toxicity

We evaluated the toxicity profile of CRLX101-based CRT by investigating hair toxicity of CRLX101-based CRT in mice. We compared the toxicity profile of combining radiotherapy with CRLX101, CPT, or PBS (control). At 49 days after irradiation, we observed hair change in 75% of CRLX101-treated animals, 100% of CPT-treated animals, and 57% of animals receiving PBS (Supplementary Fig. S2). Mice treated with either CRLX101 or PBS and radiotherapy exhibited no alopecia. In contrast, we observed alopecia in 43% of mice treated with CPT and radiotherapy (Supplementary Fig. S2).

Gastrointestinal toxicity is one of the most commonly encountered and clinically relevant toxicities experienced

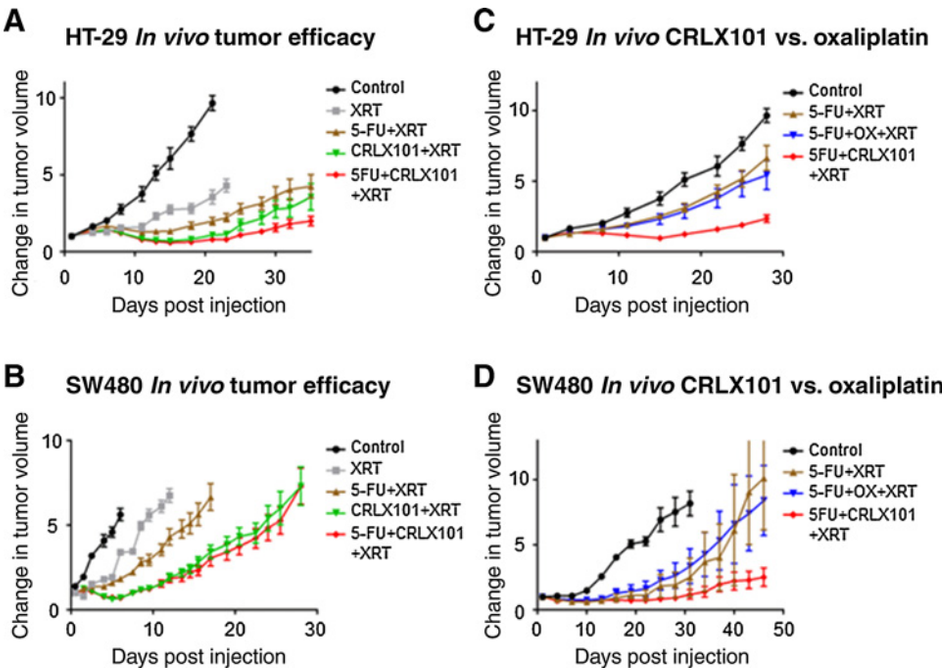

Figure 4.
Efficacy of CRLX101 CRT treatment on xenograft growth rates *in vivo*. Growth rates of HT-29 (**A**) and SW480 (**B**) tumor xenografts treated with radiation and 5-FU and/or CRLX101. Growth rates of HT-29 (**C**) and SW480 (**D**) tumor xenografts treated with 5-FU CRT and CRLX101 or oxaliplatin (OX).

during CRT in rectal cancer patients. To evaluate GI toxicity, we quantified the number of cells undergoing radiation-induced apoptosis in the colonic tissues of animals receiving PBS, CPT, or CRLX101 and fractionated radiation (5 Gy × 3) by immunostaining for cleaved caspase-3, a marker of apoptosis. We found that animals treated with radiotherapy and CPT or CRLX101 demonstrated higher GI toxicities than animals treated with radiation only. Importantly, the GI toxicity observed in animals treated with radiotherapy and CRLX101 was significantly lower than that in animals treated with radiotherapy and CPT (Fig. 6A). Notably, animals in all treatment arms demonstrated normal colonic morphology at 14 days after treatment (Fig. 6B).

Discussion

The recent development of CRLX101, a nanoparticle–drug conjugate containing CPT as the payload, offers a unique opportunity to revisit the use of topo-1 inhibitors in CRT for rectal cancer treatment. This development may facilitate the clinical translation of CPT into CRT regimens for rectal cancer. Clinical trials have demonstrated that CRLX101 has a favorable toxicity profile and its dual function (inhibition of both topo-1 and HIF1α) makes it a promising radiosensitizer for use in CRT.

Although CPT is known to be a potent radiosensitizer (37), incorporation of CPT into a nanoparticle formulation may affect its radiosensitizing efficacy. Hence, we first examined the potency of CRLX101 as a radiosensitizer *in vitro*. We found that CRLX101 is as effective as free CPT at radiosensitizing rectal cancer cells *in vitro*. We did not find CRLX101 to be superior to CPT in *in vitro* radiosensitization, because the EPR effect is an *in vivo* phenomenon. Inhibition of post-radiation DNA repair is one mechanism responsible for radiosensitization. CPT is known to promote radiosensitization by inhibiting topo-1 and directly causing DNA damage while preventing successful DNA repair. Consistent with this mechanism, we found that CRLX101 promotes radiosensitization in part by promoting the formation and persistence of radiation induced DSBs. Another mechanism for promoting radiosensitization is by inhibiting prosurvival pathways. Given that radiotherapy is known to induce HIF1α signaling, a pathway that promotes radioresistance in cancer cells (25, 38), we examined the effect of CRLX101 on HIF1α activity following radiation damage. Consistent with previous studies investigating the effects of combining CRLX101 with bevacizumab, our data showed that CRLX101 inhibits HIF1α upregulation in a prolonged manner (38). Importantly, HIF1α inhibition resulted in reduced expression of downstream HIF1α signaling targets, including CAIX and VEGF (25). Although both CPT and CRLX101 inhibit radiation induced HIF1α expression, CRLX101 led to a more sustained inhibition of HIF1α expression, likely due to prolonged CPT release.

Because HIF1α has been implicated in promoting resistance to radiotherapy (34), the ability of CRLX101 to inhibit HIF1α in addition to topo-1 has the potential of increasing the efficacy of rectal cancer CRT. We validated our *in vitro* findings using a subcutaneous mouse xenograft model of rectal cancer, a model that has been widely used in preclinical studies. We demonstrated that CRLX101 is indeed a potent radiosensitizer *in vivo*. We also found that in HT-29 and SW480 xenografts, the administration of a CRT regimen containing both 5-FU and CRLX101 had the highest therapeutic efficacy. This finding suggests that the optimal CRT regimen for rectal cancer treatment should include both CRLX101 and 5-FU. We hypothesized that 5-FU enhanced the efficacy of CRLX101-based CRT by preventing accelerated repopulation inhibition. Accelerated repopulation following radiotherapy is a well-known phenomenon that contributes to the local recurrence of tumors (39). During accelerated repopulation, growth-stimulating signals from dying cells promote rapid proliferation of surviving tumor cells after treatment (36, 40). To examine this possibility, we utilized an established

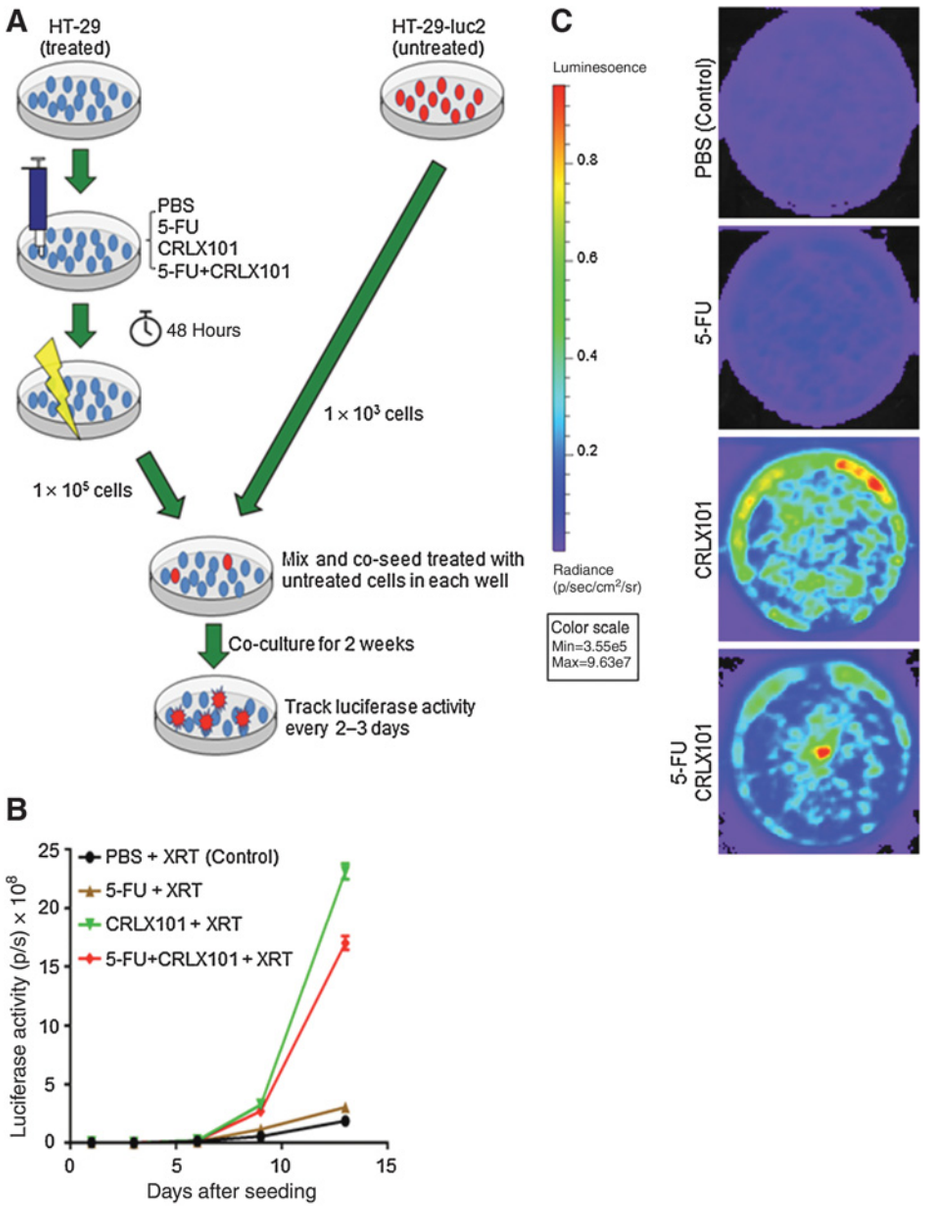

Figure 5.
Effect of CRLX101 on colorectal cancer cell repopulation. **A,** Schematic drawing of *in vitro* cell repopulation assay. **B,** Quantification of untreated HT-29-luc2 cell growth over time following treatment with radiation (XRT) and PBS (control), 5-FU, CRLX101, or 5-FU, and CRLX101. **C,** Representative bioluminescence images of HT-29-luc2 cell cultures 13 days following treatment.

repopulation assay and found that while CRLX101-based CRT treatment promoted accelerated repopulation, the addition of 5-FU to CRLX101-based CRT negated this effect. These data suggest that 5-FU acts synergistically with CRLX101 *in vivo* to suppress tumor growth after CRT by inhibiting accelerated repopulation. Taken together, these preclinical findings support the clinical use of CRT treatment regimens that contain both 5-FU and CRLX101.

Although promising in preclinical studies, clinical trials investigating the use of oxaliplatin in rectal cancer CRT have not shown sufficient enhancement of CRT efficacy to support its use. Consistent with previous data, the addition of oxaliplatin to 5-FU–based CRT did not improve therapeutic efficacy in our mouse xenograft model of rectal cancer. Importantly, we found that combining radiotherapy with CRLX101 and 5-FU is significantly more effective than combining radiotherapy with oxaliplatin and 5-FU. These *in vivo* results provide strong evidence to support clinical testing of CRLX101 as an additive to standard rectal cancer CRT. While these results are encouraging, it is important to point out that other factors, such as chemotherapeutic bioavailability, may have influenced the outcome of this preclinical study.

Lastly, we also examined the potential toxicity of CRLX101-based CRT to normal tissues *in vivo*. Radiation elevates vascular permeability within both tumor and normal tissues (41–43). We assessed the effect that adding CRLX101 to radiotherapy had on GI toxicity by examining apoptosis rates in colonic tissues shortly following radiation damage. We found that the addition of CRLX101 to radiotherapy resulted in lower rates of radiation-induced apoptosis when compared with animals treated with CPT and radiotherapy. There was, however, some evidence of GI toxicity in animals treated with CRLX101 and radiotherapy, possibly due to increased vascular permeability

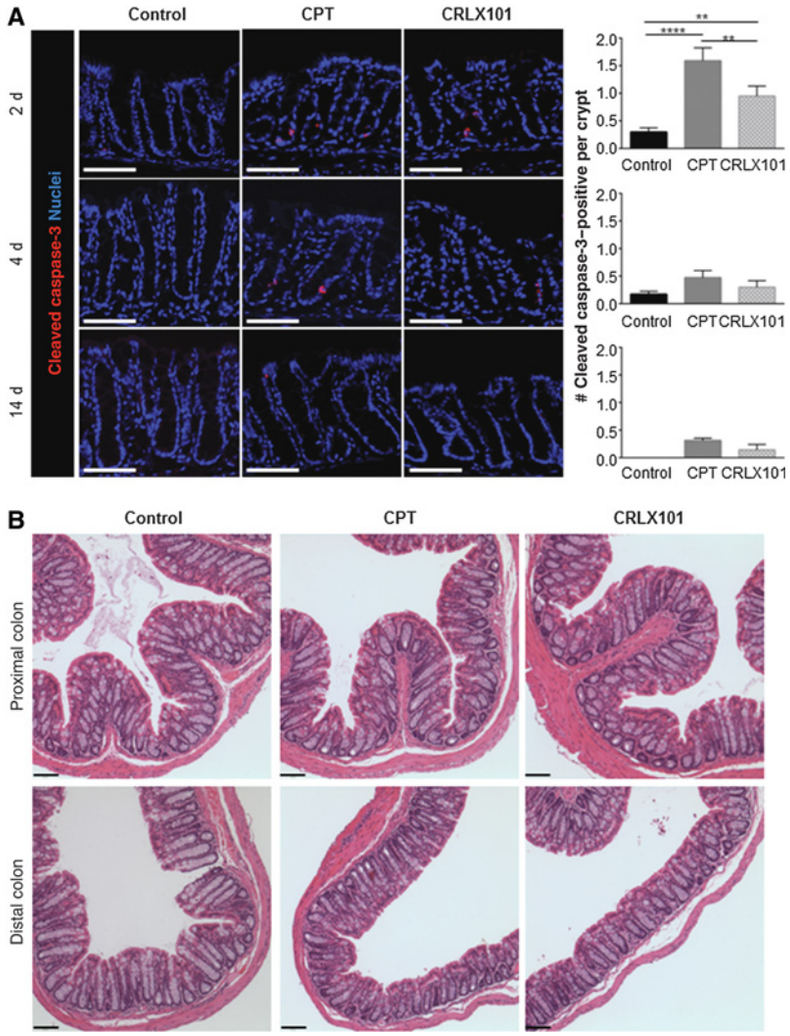

Figure 6.

Evaluation of GI toxicity following CRLX101 treatment. **A,** Representative images and quantification of cleaved caspase-3 immunofluorescence in distal colon over time following treatment with PBS (control), CPT, or CRLX101, and radiation. Scale bar, 50 μm. **, $P < 0.01$; ****, $P < 0.0001$. **B,** Representative images of hematoxylin and eosin staining depicting global proximal and distal colonic morphology 14 days after treatment with PBS (control), CPT, or CRLX101, and radiation. Scale bar, 80 μm.

following radiation damage. In addition to evaluating GI toxicity, we also evaluated mouse hair toxicity as a surrogate for skin and mucosal surface toxicity. We demonstrated that while the addition of CRLX101 did increase hair toxicity, the effect is mild. We hypothesize that this finding will not be clinically significant.

In summary, these preclinical data demonstrate that CRLX101 is a potent radiosensitizer with the potential of improving rectal cancer CRT. CRLX101 functions by inhibiting both topo-1 and the HIF1α signaling. Our data indicate that CRLX101 and 5-FU may be an optimal CRT regimen for rectal cancer treatment. Our preclinical data support the ongoing phase Ib/II clinical trial, LCCC1315, titled "Neoadjuvant Chemoradiotherapy with CRLX-101 and Capecitabine for Rectal Cancer" (ClinicalTrials.gov Identifier: NCT02010567).

Disclosure of Potential Conflicts of Interest

E.G. Garmey is chief medical officer at Cerulean Pharma Inc. and has ownership interest (including patents) in the same. J.E. Tepper reports receiving a commercial research grant from Cerulean. S. Eliasof is vice president, research, at Cerulean Pharma Inc. and has ownership interest (including patents) in the same. A.Z. Wang reports receiving a commercial research grant from Cerulean Pharma. No potential conflicts of interest were disclosed by the other authors.

Authors' Contributions

Conception and design: X. Tian, M. Nguyen, J.M. Caster, E.G. Garmey, J.E. Tepper, S. Eliasof, A.Z. Wang

Development of methodology: X. Tian, M. Nguyen, H.P. Foote, K.C. Roche, E.G. Garmey, A.Z. Wang

Acquisition of data (provided animals, acquired and managed patients, provided facilities, etc.): X. Tian, M. Nguyen, H.P. Foote, J.M. Caster, K.C. Roche, C.G. Peters, P. Wu, L. Jayaraman, A.Z. Wang

Analysis and interpretation of data (e.g., statistical analysis, biostatistics, computational analysis): X. Tian, M. Nguyen, H.P. Foote, J.M. Caster, C.G. Peters, P. Wu, L. Jayaraman, E.G. Garmey, A.Z. Wang
Writing, review, and/or revision of the manuscript: X. Tian, M. Nguyen, J.M. Caster, K.C. Roche, L. Jayaraman, E.G. Garmey, J.E. Tepper, S. Eliasof, A.Z. Wang
Administrative, technical, or material support (i.e., reporting or organizing data, constructing databases): M. Nguyen, A.Z. Wang
Study supervision: L. Jayaraman, A.Z. Wang

Acknowledgments

We would like to give special thanks to Kyle Wagner for tumor measurement and Jonathan Frank for bioluminescence analysis.

Grant support

This work was supported by the University Cancer Research Fund from the University of North Carolina to A.Z. Wang and R01CA178748, U54CA151652, and U54CA198999 from the NIH/NCI to A.Z. Wang.

The costs of publication of this article were defrayed in part by the payment of page charges. This article must therefore be hereby marked *advertisement* in accordance with 18 U.S.C. Section 1734 solely to indicate this fact.

Received October 26, 2015; revised October 13, 2016; accepted October 21, 2016; published OnlineFirst October 26, 2016.

References

1. Siegel R, DeSantis C, Virgo K, Stein K, Mariotto A, Smith T, et al. Cancer treatment and survivorship statistics, 2012. CA Cancer J Clin 2012;62: 220–41.
2. Minsky BD, Cohen AM, Kemeny N, Enker WE, Kelsen DP, Reichman B, et al. Combined modality therapy of rectal cancer: decreased acute toxicity with the preoperative approach. J Clin Oncol 1992;10: 1218–24.
3. Sauer R, Liersch T, Merkel S, Fietkau R, Hohenberger W, Hess C, et al. Preoperative versus postoperative chemoradiotherapy for locally advanced rectal cancer: results of the German CAO/ARO/AIO-94 randomized phase III trial after a median follow-up of 11 years. J Clin Oncol 2012; 30:1926–33.
4. Tepper JE, O'Connell MJ, Petroni GR, Hollis D, Cooke E, Benson AB 3rd, et al. Adjuvant postoperative fluorouracil-modulated chemotherapy combined with pelvic radiation therapy for rectal cancer: initial results of intergroup 0114. J Clin Oncol 1997;15:2030–9.
5. Krook JE, Moertel CG, Gunderson LL, Wieand HS, Collins RT, Beart RW, et al. Effective surgical adjuvant therapy for high-risk rectal carcinoma. N Engl J Med 1991;324:709–15.
6. Fisher B, Wolmark N, Rockette H, Redmond C, Deutsch M, Wickerham DL, et al. Postoperative adjuvant chemotherapy or radiation therapy for rectal cancer: results from NSABP protocol R-01. J Natl Cancer Inst 1988;80:21–9.
7. Sauer R, Becker H, Hohenberger W, Rodel C, Wittekind C, Fietkau R, et al. Preoperative versus postoperative chemoradiotherapy for rectal cancer. N Engl J Med 2004;351:1731–40.
8. Willett CG, Duda DG, Ancukiewicz M, Shah M, Czito BG, Bentley R, et al. A safety and survival analysis of neoadjuvant bevacizumab with standard chemoradiation in a phase I/II study compared with standard chemoradiation in locally advanced rectal cancer. Oncologist 2010; 15:845–51.
9. Willett CG, Duda DG, di Tomaso E, Boucher Y, Ancukiewicz M, Sahani DV, et al. Efficacy, safety, and biomarkers of neoadjuvant bevacizumab, radiation therapy, and fluorouracil in rectal cancer: a multidisciplinary phase II study. J Clin Oncol 2009;27:3020–6.
10. Crane CH, Eng C, Feig BW, Das P, Skibber JM, Chang GJ, et al. Phase II trial of neoadjuvant bevacizumab, capecitabine, and radiotherapy for locally advanced rectal cancer. Int J Radiat Oncol Biol Phys 2010; 76:824–30.
11. Wong SJ, Winter K, Meropol NJ, Anne PR, Kachnic L, Rashid A, et al. Radiation Therapy Oncology Group 0247: a randomized Phase II study of neoadjuvant capecitabine and irinotecan or capecitabine and oxaliplatin with concurrent radiotherapy for patients with locally advanced rectal cancer. Int J Radiat Oncol Biol Phys 2012;82:1367–75.
12. Aschele C, Cionini L, Lonardi S, Pinto C, Cordio S, Rosati G, et al. Primary tumor response to preoperative chemoradiation with or without oxaliplatin in locally advanced rectal cancer: pathologic results of the STAR-01 randomized phase III trial. J Clin Oncol 2011;29:2773–80.
13. Ryan DP, Niedzwiecki D, Hollis D, Mediema BE, Wadler S, Tepper JE, et al. Phase I/II study of preoperative oxaliplatin, fluorouracil, and external-beam radiation therapy in patients with locally advanced rectal cancer: Cancer and Leukemia Group B 89901. J Clin Oncol 2006;24:2557–62.
14. de Campos-Lobato LF, Stocchi L, da Luz Moreira A, Geisler D, Dietz DW, Lavery IC, et al. Pathologic complete response after neoadjuvant treatment for rectal cancer decreases distant recurrence and could eradicate local recurrence. Ann Surg Oncol 2011;18:1590–98.
15. Park IJ, You YN, Agarwal A, Skibber JM, Rodriguez-Bigas MA, Eng C, et al. Neoadjuvant treatment response as an early response indicator for patients with rectal cancer. J Clin Oncol 2012;30:1770–6.
16. Young C, Schluep T, Hwang J, Eliasof S. CRLX101 (formerly IT-101)—a novel nanopharmaceutical of camptothecin in clinical development. Curr Bioact Compd 2011;7:8–14.
17. Habr-Gama A, Perez RO, Sao Juliao GP, Proscurshim I, Gama-Rodrigues J. Nonoperative approaches to rectal cancer: a critical evaluation. Semin Radiat Oncol 2011;21:234–9.
18. Tepper JE, Wang AZ. Improving local control in rectal cancer: radiation sensitizers or radiation dose? J Clin Oncol 2010;28:1623–4.
19. Rodel C, Liersch T, Becker H, Fietkau R, Hohenberger W, Hothorn T, et al. Preoperative chemoradiotherapy and postoperative chemotherapy with fluorouracil and oxaliplatin versus fluorouracil alone in locally advanced rectal cancer: initial results of the German CAO/ARO/AIO-04 randomised phase 3 trial. Lancet Oncol 2012;13:679–87.
20. Mehta VK, Cho C, Ford JM, Jambalos C, Poen J, Koong A, et al. Phase II trial of preoperative 3D conformal radiotherapy, protracted venous infusion 5-fluorouracil, and weekly CPT-11, followed by surgery for ultrasound-staged T3 rectal cancer. Int J Radiat Oncol Biol Phys 2003; 55:132–7.
21. Klautke G, Feyerherd P, Ludwig K, Prall F, Foitzik T, Fietkau R. Intensified concurrent chemoradiotherapy with 5-fluorouracil and irinotecan as neoadjuvant treatment in patients with locally advanced rectal cancer. Br J Cancer 2005;92:1215–20.
22. Glynne-Jones R, Falk S, Maughan TS, Meadows HM, Sebag-Montefiore D. A phase I/II study of irinotecan when added to 5-fluorouracil and leucovorin and pelvic radiation in locally advanced rectal cancer: a Colorectal Clinical Oncology Group Study. Br J Cancer 2007;96:551–8.
23. Chen AY, Choy H, Rothenberg ML. DNA topoisomerase I-targeting drugs as radiation sensitizers. Oncology 1999;13:39–46.
24. Eliasof S, Lazarus D, Peters CG, Case RI, Cole RO, Hwang J, et al. Correlating preclinical animal studies and human clinical trials of a multifunctional, polymeric nanoparticle. Proc Natl Acad Sci U S A 2013;110:15127–32.
25. Moeller BJ, Cao Y, Li CY, Dewhirst MW. Radiation activates HIF-1 to regulate vascular radiosensitivity in tumors: role of reoxygenation, free radicals, and stress granules. Cancer Cell 2004;5:429–41.
26. Gaur S, Chen L, Yen T, Wang Y, Zhou B, Davis M, et al. Preclinical study of the cyclodextrin–polymer conjugate of camptothecin CRLX101 for the treatment of gastric cancer. Nanomedicine 2012;8:721–30.
27. Weiss GJ, Chao J, Neidhart JD, Ramanathan RK, Bassett D, Neidhart JA, et al. First-in-human phase 1/2a trial of CRLX101, a cyclodextrin-containing polymer-camptothecin nanopharmaceutical in patients with advanced solid tumor malignancies. Invest New Drug 2013;31:986–1000.
28. Hobbs SK, Monsky WL, Yuan F, Roberts WG, Griffith L, Torchilin VP, et al. Regulation of transport pathways in tumor vessels: role of tumor type and microenvironment. Proc Natl Acad Sci U S A 1998; 95:4607–12.
29. Jain RK, Stylianopoulos T. Delivering nanomedicine to solid tumors. Nat Rev Clin Oncol 2010;7:653–64.
30. Svenson S, Wolfgang M, Hwang J, Ryan J, Eliasof S. Preclinical to clinical development of the novel camptothecin nanopharmaceutical CRLX101. J Control Release 2011;153:49–55.

31. Schluep T, Cheng J, Khin KT, Davis ME. Pharmacokinetics and biodistribution of the camptothecin-polymer conjugate IT-101 in rats and tumor-bearing mice. Cancer Chemother Pharmacol 2006;57: 654–62.
32. Karve S, Werner ME, Sukumar R, Cummings ND, Copp JA, Wang EC, et al. Revival of the abandoned therapeutic wortmannin by nanoparticle drug delivery. Natl Acad Sci U S A 2012;109:8230–5.
33. Semenza GL.Intratumoral hypoxia, radiation resistance, and HIF-1. Cancer Cell 2004;5:405–6.
34. Harada H, Inoue M, Itasaka S, Hirota K, Morinibu A, Shinomiya K, et al. Cancer cells that survive radiation therapy acquire HIF-1 activity and translocate towards tumour blood vessels. Nature Commum 2012;3: 783.
35. Potter C, Harris AL. Hypoxia inducible carbonic anhydrase IX, marker of tumour hypoxia, survival pathway and therapy target. Cell Cycle 2004; 3:164–7.
36. Donato AL, Huang Q, Liu X, Li F, Zimmerman MA, Li CY. Caspase 3 promotes surviving melanoma tumor cell growth after cytotoxic therapy. J Invest Dermatol 2014;134:1686–92.
37. Kim JH, Kim SH, Kolozsvary A, Khil MS. Potentiation of radiation response in human carcinoma cells in vitro and murine fibrosarcoma in vivo by topotecan, an inhibitor of DNA topoisomerase I. Int J Radiat Oncol Biol Phys 1992;22:515–8.
38. Pham E, Birrer MJ, Eliasof S, Garmey EG, Lazarus D, Lee CR, et al. Translational impact of nanoparticle–drug conjugate CRLX101 with or without bevacizumab in advanced ovarian cancer. Clin Cancer Res 2015; 21:808–18.
39. Hittelman WN, Liao Y, Wang L, Milas L. Are cancer stem cells radio-resistant? Future Oncol 2010;6:1563–76.
40. Huang Q, Li F, Liu X, Li W, Shi W, Liu FF, et al. Caspase 3-mediated stimulation of tumor cell repopulation during cancer radiotherapy. Nat Med 2011;17:860–6.
41. Park HJ, Griffin RJ, Hui S, Levitt SH, Song CW. Radiation-induced vascular damage in tumors: implications of vascular damage in ablative hypofractionated radiotherapy (SBRT and SRS). Radiat Res 2012;177: 311–27.
42. Willoughby DA. Pharmacological aspects of the vascular permeability changes in the rat's intestine following abdominal radiation. Br J Radiol 1960;33:515–9.
43. Park KR, Monsky WL, Lee CG, Song CH, Kim DH, Jain RK, et al. Mast cells contribute to radiation-induced vascular hyperpermeability. Radiat Res 2016;185:182–9.